

Vector Field Convolution for Segmentation and Measurement of Pleural Effusion

B.S.Lijin, S. Malathi, G. Arun Kumar, S.ManiKandan

Final Year Student, Dept of Computer Science and Engineering, Panimalar Engineering College, Chennai, India.

Final Year Student, Dept of Computer Science and Engineering, Panimalar Engineering College, Chennai, India.

Professor, Dept of Computer Science and Engineering, Panimalar Engineering College, Chennai, India.

Abstract— Pleural effusion is a vital biomarker for the diagnosis of many diseases. A pleural effusion is an anomalous amount of fluid around the lung that can result from many medical conditions. In this paper, an improved automated method is implemented to evaluate pleural effusion on CT scan and prohibitively time consuming when performed manually. The proposed method is based on parietal pleura extraction and visceral pleura extraction and active contour external force using vector field convolution for image segmentation along with region growing and Bezier surface fitting and deformable surface modeling. Twelve CT scans with three manual segmentation were used to evaluate the automatic segmentation method. The visceral assessment estimated 85% cases with negligible or small segmentation errors 13% with medium errors and 2% with large errors.

Keywords— pleural effusion, vector field convolution, deformable surface modeling

I. INTRODUCTION

Pleural effusion buildups of fluid within the pleural cavity, are usually a symptom of a greater illness such as congestive heart failure, pneumonia, or metastatic cancer[1]. Excessive accumulation of pleural fluid can compress the underlying lung and result in impaired ventilation, resultant shortness of breath, increased susceptibility to superimposed infection. The amount of pleural fluid is difficult clinically due to complex topology of pleural cavity but is important for decision making regarding the need for removing the fluid via chest pain(pleurodesis). It is important for the monitoring the success of medical therapy. PE can be formed in two ways transudates where the fluid is pushed into the pleural space from elsewhere due to changes in hydrostatic pressure and exudates where the fluid is created by the pleural surface itself.

M.R. Thansekhar and N. Balaji (Eds.): ICIET'14

Computed tomography (CT) can readily demonstrate small amounts of fluid in either the pleural space or peritoneum. The differentiation of the ascities from pleural effusion by CT can be difficult [21]. The report of a retrospective analysis of CT examination has described the four specific criteria namely, the diaphragm sign, displaced crus sign, interface sign and the bare sign. Ascities can be readily differentiated from pleural effusion by the use of the diaphragm sign.

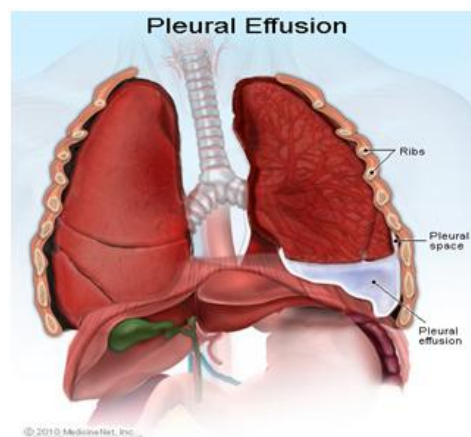


Fig.1 Graphical representation of section of lungs for clear visualization of Pleural Effusion

PEs can be detected via a number of invasive methods including chest radiographs and computed tomography (CT) Chest studies and ultrasound (US).CT is increasing replacing chest radiographs as the dominant method to measure PEs.Diagnosis of pleural effusion was based on clinical examination and chest radiography. Chest

ultrasonography with better sensitivity and reliability in the diagnosis of pleural effusions than chest x-ray can be repeated serially without any radiation risk.

Chest drainage was indicated and considered as potentially useful for the patient. Sonograms were before drainage at the bedside, in supine position and measurement were performed at the end of expiration. Effusion were classified as >500 mL or ≤ 500 mL according to drained volume [4]. Though US radiography, and CT can all be used in manual estimation of effusion size and no fully automated currently exist that can segment and measure PEs.

A few more automated methods had also been proposed used a slice-by slice constrained region based segmentation can also segment pulmonary masses. A novel slice-by-slice code is presented which performs conditional region growth to accurately segment the effusion space. In that section II specifies related work and further, section III contain project work. Section IV contain result and description and section V contain conclusion

II. RELATED WORK

J. Manuel Porcel et.al, proposed paper [2] to report the etiology of large and massive pleural effusion, and to compare their biochemical fluid characteristics with those of smaller size, and between malignant and non-malignant conditions. Since the presence of a large or massive pleural effusion enables the clinician narrow the differential diagnosis of pleurisy, since most effusion or secondary to malignancy or infections. Bloody pleural fluid with low ADA content favors a malignant condition. The various positions has been tried to find out which position is suitable for detecting pleura in lungs, among that various prospective analysis of anteroposterior supine radiograph to determine the detectability pleural effusion on supine radiographs. The routine use of supine positioning for portable chest radiographs is controversial. Although the supine radiographs are easier to take and potentially more reproducible, the accuracy of pleural effusion. The supine radiographs are moderately sensitive and specific for the evaluation of pleural effusion the value of supine chest examination for routine has not been determine.

Ultrasound has used instead of x-ray to detect pleura in lung ultrasound is mainly used in mechanically ventilated patients. The patients with incomplete aspiration of pleural fluid on post-puncture ultrasound were excluded. Easy quantification of pleural fluid may help to decide about performing thoracentesis under ultrasound guidance appears to be a safe procedure [3]. Antoine roch proposed paper to assess the accuracy of chest ultrasonography in predicting pleural effusions > 500 ml in patients receiving mechanical ventilation. Diagnosis of pleural effusions was based on clinical examination and chest radiography, initially sonograms were performed before drainage at the bed side, in supine position. Effusions were classified as >500 mL or < 500 mL according to drained volume [5]. Finally bedside pleural ultrasonography accurately predicted a

M.R. Thansekhar and N. Balaji (Eds.): ICIET'14

nonloculated pleural effusion > 500 mL in patient's receiving mechanical ventilation using simple And reproducible measurements. Wenil Cai, et.al, proposed paper to develop and validate an automated computer aided volumetry scheme for detection and measurement of Pneumothoraces for Trauma Patients with MDCT. A computer-aided volumetry of Pneumothorax consists of five automated steps for measuring Pneumothoraces. The result show that our computer-aided volumetric scheme provides an automated method for accurate and efficient detection [6].

Constrained region-based segmentation of pleural effusion in thin-slice CT [7], addressed that measuring the fluid volume is indicative of the effectiveness of any treatment but due to the similarity to surrounded regions, fragments of collapsed lung present and topological changes. A novel slice-by-slice code is presented which performs conditional region growth to accurately segment the effusion shape. In this paper several problems found that is an accurate comparison between these volume calculations and effusion volumes estimated manually. This will include a measure of the spread of manual methods compared to our approach. The various new method was developed for quantification of pleural effusion from CT image, a various crucial pretreatment of computing the volume of pleural effusion [8] is to segment an extract the effusion efficiently, cube hermite curve fitting and bounding box technology has used detect boundary points to be identified automatically, tangents of boundary points estimated by Bessel method and the construction of pleural contour can applied to computing pleural volume.

A balloon model is introduced by Laurent D, et.al, to generalize and solve some of problems encountered with the original method, Balloons is deformed under the action of internal and external forces attracting the surface toward detected edges by means of an attraction potentials, using a series of 2-D contours in successive cross section to make a 3-D reconstruction of the surface of ventricles [9]. Another method, was introduced a new region growing method for segmenting medical images. This region growing method uses a closed snake driven by pressure forces [10], the pressurized snakes have been used to reconstruct various anatomical objects from medical images. Modeling a deformable contour from noisy images, uses a global contour model which is invariant and unique, combined with markov random field to model local deformations.

III. PROPOSED WORK

We used routine CT scan from previous studies. the slices were 512×512 with 5mm slice thickness and in plane spacing from .63mm to .88mm. the age of the 15 patients ranged from 32 to 79 years, with the mean of 52.4 [4]. Three set of manual segmentation were generated for the 12 validation datasets. Two were produced by a research fellow, months apart. The other was produced by a professional image processing technologist. All manual segmentation was made with custom developed software.

A) Preprocessing

Preprocessing aims to reduce noise and smooth the image. In an anisotropic diffusion, an image f defined in a domain Ω , is allowed to evolve over time via the following partial differential equation [16]

$$\frac{\partial f}{\partial t} = \text{div} (c(|\nabla f|)|\nabla f) \quad (1)$$

The filter moves pixel intensities of the image without blurring edges. The filter moves pixel intensities toward the average of the surrounding regions. Diffusion coefficient $c(|\Delta f|) \in [0,1]$ is required to be a decreasing function of the magnitude of local gradient such that it diffuses more in regions of small gradients and less around edges where the gradients are large.

B) Lung segmentation

The various segmentation algorithm previously developed by use group [17]. The lung intensity can be determined by analyzing the intensity histogram using Otsu's method [18]. A rough segmentation of the lungs can be produced using 3-D region growing method

C) Visceral Pleura Detection

The visceral layer covers the inner part of the lungs and parietal layer are attached to chest wall. The pleural fluid is accumulated at the bottom of the pleural space, the visceral and parietal layer need to be extracted by using three step routine[20]. First, initial layer is detected at the boundary of lung. second, B-spline is fitted to initial layer and third a VFC is applied to refine the layer.

$$VL(x) = \text{argmax} (B(x, y)) \quad (2)$$

$$y, \text{ s. t. } B(x, y) = 1$$

$$B(x, y) = \begin{cases} 1, & \text{where } s(x, y) = 1 \text{ and } s(x, y + 1) = 0 \\ 0, & \text{otherwise} \end{cases} \quad (3)$$

Where $B(x,y)$ is the lung boundary map, $S(x,y)$ is the lung segmentation mask. Vector field convolution snakes are active contour using the VFC field as the external force. By replacing the standard external force $f_{\text{ext}}(v) = -E_{\text{ext}}(v)$ by the VFC field $f_{\text{VFC}}(v)$ the iterative snakes solution

The static external forces called Vector field convolution [9] is introduced, first define a vector field kernel $k(x, y) = [u_k(x, y), v_k(x, y)]$ In which all the vector point to kernel origin.

$$k(x, y) = m(x, y), n(x, y) \quad (4)$$

Where $m(x,y)$ is magnitude of the vector at (x,y) , $n(x,y)$ is unit vector pointing to kernel origin $(0,0)$

$$N(x, y) = \left[\frac{-x}{r}, \frac{-y}{r} \right] \quad (5)$$

VFC external force $F_{\text{VFC}}(x,y) = [u_{\text{VFC}}(x,y), v_{\text{VFC}}(x,y)]$ is given by calculating the convolution of the vector field $k(x,y)$ and the edge map $f(x,y)$ generated from image $I(x,y)$

$$F_{\text{VFC}} = f(x, y) * k(x, y) = [f(x, y) * u_k(x, y), f(x, y) * v_k(x, y)] \quad (6)$$

The edge map is non negative and larger near the image edges, edges contribute more to the VFC than homogeneous regions. therefore the VFC external force will attract free particles to the edges. VFC field highly depends on the magnitude should be decreasing positive function of distance from the origin. In that we propose two types of magnitude function given as

$$M_1(x, y) = (r + \epsilon)^{-\gamma} \quad (7)$$

$$M_2(x, y) = \exp\left(\frac{-r^2}{\zeta}\right) \quad (8)$$

Where γ and ζ are positive parameters to control the decrease ϵ is a small constant to prevent division by zero at the origin

D) Parietal Pleura Detection:

The parietal layer is detection is identified using a similar three step routine for the parietal extraction. First, landmark points the inner rib cage is detected and Bernstein polynomial is fitted to it and VCF active contour is applied to refine the layer. The algorithm identifies points of high intensity. The difference in intensity gradient between its anterior and posterior, such that those borders line up with edges of the bone.

E) PE surface Fitting :

The endpoints of the curves produced with connected straight lines to form a closed shape and all the pixels that fall inside are defined as PE using a scanline algorithm. The pleural space is segmented are evenly sampled (250 samples points). Sample points are used as control points to generate a Bezier surface

$$P(u, v) = \sum_{i=0}^n \sum_{j=0}^m Z_i^n(u) Z_j^m(v) k_{i,j} \quad (9)$$

where $p(u,v)$ is a point on the surface is the degree of the surface, which varies with the number of control points and Z is the Bezier surface function, $k_{i,j}$ is the set of control points

F) Three- Dimensional Deformable Modeling :

Deformable surface is the applied to refine the boundary of PE using vector field convolution [12]. The model is driven by an external image forces and internal forces. An active contour deforms through the image to minimize the energy

$$E_{AC} = \int_0^1 \left[\frac{1}{2} (\alpha |x'(s)|)^2 + (\beta |x''(s)|)^2 + E_{\text{ext}}(x(s)) \right] ds \quad (10)$$

Where α and β are parameters represents the smoothness and tautness degree of contour and $x'(s)$ and $X''(s)$ are first and second derivatives of $x(s)$ and E_{ext} represents the external energy

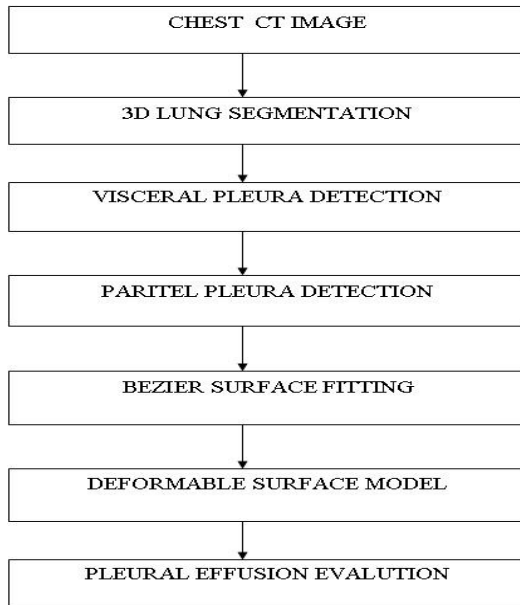


Fig.2 Schematic of the automatic pleural effusion Evaluation process

Initially chest ct image is give as input, where segmentation of lungs has been obtained where visceral pleura layer and paritel layer are detected ,Bezier surface fitting used to obtain a deformable surface model is obtained ,from that pleural effusion is evaluated

IV. RESULT AND DESCRIPTION

TABLE I

Table 1 shows comparisons made between manual segmentation, automatic segmentation by VFC and segmentation using ACM

CT Scan	Auto	Manual 1	Manual 2	ACM
1	250	255	251	245
2	433	435	431	428
3	385	378	375	365

Table 1 depicts the comparison of volume of pleural effusion in different segmentation techniques, compared active contour model, VFC gives more less equivalent value which was already found by experienced radiologist

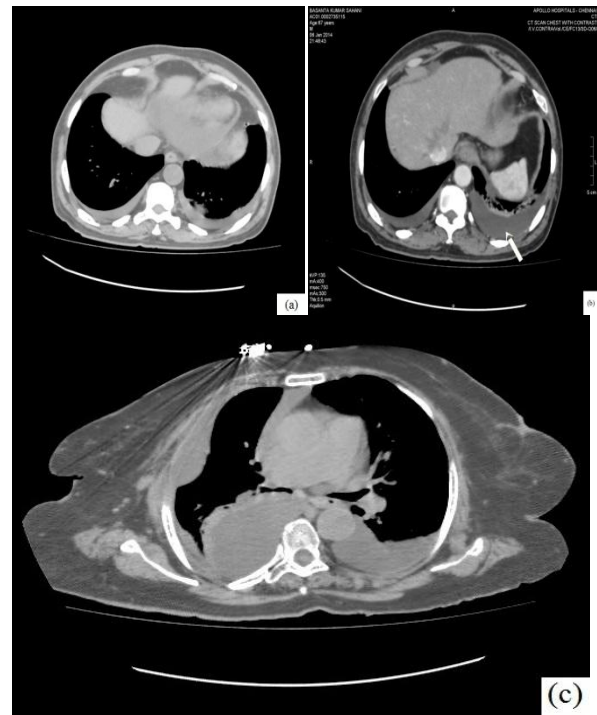


Fig 2: a) lungs without pleural effusion b) lungs with massive pleural effusion c) anteroposterior position of lungs

The paper works with pleural effusions have specific shape, start on the posterior side of lung before its interior and extend downward without moving in anterior direction, bottom of the lung. In the previous version's segmentation include too much tissue which inhibits the vector field convolution algorithm ability to identify a good threshold

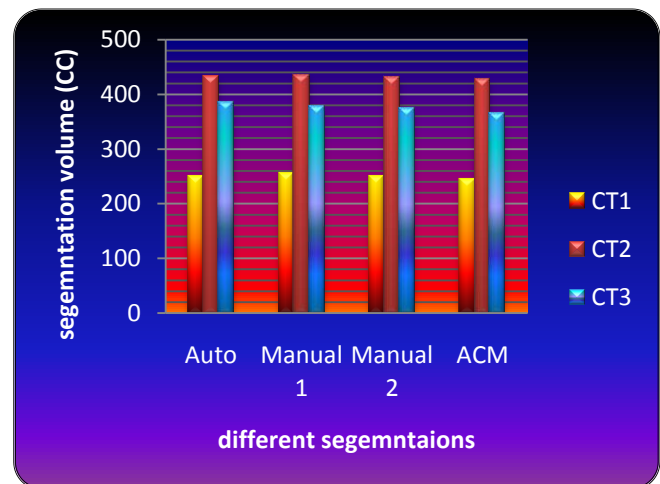


Fig 3: Comparisons of correlations pleural effusion volume estimates

Fig 3 depicts by using data from the table that by comparing the automatic segmentation by vector field convolution and manual segmentation ,manual 1 depicts the manual segmentation of experienced radiologist where manual 2 shows the manual segmentation of inexperienced radiologist and in ACM shows the previous segmentation technique

IV. CONCLUSION

The program works best with PEs which have specific shape, they start on posterior side of the lungs and extend in the inferior direction without moving far in anterior direction below the bottom of the lung. In this paper, a novel static external force active contour called vector field convolution (VFC) has been introduced. The VFC field is calculated by convolving vector field kernel with edge map generated from the image. The main reason to eliminate outliers caused by shoulder bones and leakage since .Bezier surface was used for the 3-D surface modeling of PE since its numerically stable and robust to control point selection. We used VFC to further refine the segmentation of the visceral layer due to its effectiveness

REFERENCES

[1] R.W Light, "Pleural effusion," *New Eng.J.Med.*, vol.346, pp. 1971-1972,2002

[2] J. Porcel and M. Vives, "Etiology and pleural fluid characteristics of large and massive effusions," *Chest*, vol. 124, pp. 978–983, 2003.

[3] J. A. Ruskin, J. W. Gurney, M. K. Thorsen, and L. R. Goodman, "Detection of pleural effusions on supine chest radiographs," *Amer. J.Roentgenol.*, vol. 148, pp. 681–683, 1987

[4] A.Roch, M.Bojan,P.Michelet ,F.Romain, F.Bregeon, L.Papazian and J-P Auffray Usefullness of ultrasonography in predicting pleural effusions >500 ml in patients receiving mechanical ventilation , "*Chest*, vol.127,pp.224-232,2005

[5] P. Vignon, C. Chastagner, V. Berkane, E. Chardac, B. Francois,S. Normand, M. Bonnivard, M. Clavel, N. Pichon, P. M. Preux,A. Maubon, and H. Gastinne, "Quantitative assessment of pleural effusion in critically ill patients by means of ultrasonography," *Crit. Care Med.*, vol. 33, pp. 1757–1763, 2005.

[6] W. Cai, M. Tabbara, N. Takata, H. Yoshida, G. J. Harris, R. A. Novelline, and M. de Moya, "MDCT for automated detection and measurement of pneumothoraces in trauma patients," *Amer. J. Roentgenol.*, vol. 192, pp. 830–836, 2009

[7] R. Donohue, A. Shearer, and J. Bruzzi, "Constrained region-based segmentation of pleural effusion in thin-slice CT," in *Proc. IEEE 13th Int.Mach. Vis. Image Process. Conf.*, 2009, pp. 24–29.

[8] Y. Qian, C. Zhang, and X. Yang, "New method for quantification of pleural effusions from CT imaging," in *Proc. ISECS Int. Colloq. Comput.Commun. Control Manage.*, 2008, pp. 768–773.

[9] L. D. Cohen and I. Cohen, "Finite-element methods for active contour models and balloons for 2-D and 3-D images," *IEEE Trans. Pattern Anal. Mach. Intell.*, vol. 15, no. 11, pp. 1131–1147, Nov. 1993

[10] J.Ivins and J.Porrill , "Active region segmenting medical images"Artificial intelligence vision research unit, vol.94.1994

[11] G. Sapiro , "vector – valued Active contour" *IEEE* Vol 96.1996

[12] C. Xu and J. L. Prince, "Generalized gradient vector flow external forces for active contours," *Signal Process.*, vol. 71, pp. 131–139, 1998.

[13] A. Chakraborty, L.H.Staib, and J.S. Duncan , "Deformable boundary finding in medical images by integrating gradient and region information " *IEEE Trans. Med.Image .*,vol.15 no.6, pp.859-870, dec.1996

[14] B.Fischl and E.L.Schwartz "Learning an integral equation approximation to nonlinear anisotropic diffusion in image processing " *IEEE Trans.Mach Intell.*,vol 19, No 4,1997

[15]S. T. Acton, "Multigrid anisotropic diffusion," *IEEE Trans. ImageProcess.*, vol. 7, no. 3, pp. 280–291, Mar. 1998

[16] J. Weickert *Anistropic Diffusion in image processing* . Stuttgart,Germany: B.G Teubner,1998

[17] J.Yao, A.Dwyer ,R.M.Summers and D.J .Mollura," Computer – aided diagnosis of pulmonary infections using texture analysis and support vector machine Classification " *Acad.Radiol.*, Vol.18, no. 3, pp.306-314, 2011

[18] N.Otsu , " A threshold selection method from gray –level histogram," *IEEETrans.Syst .,Man., Cybern.* ,vol.9, no.1, pp.62-66 , jan.1979

[19] J.Rogowska,"Overview and fundamentals of medical image segmentaion ," in *Handbook of Medical Imaging ,Processing and*

Analysis,I.N. Bankman, Ed. New York, NY, USA: Academic ,2000,pp.69-85

[20] A.R. Mansouri .D.P .Mukherjee,a and S.T.Acton," Constraining active contour evolution via lie gropus of transformation ," *IEEE Trans .Image.*, vol 21, no.6, pp.853-863,jun.2004

[21] R. Halvorsen, P. J. Fedyshin, M. Korobkin, W. L. Foster Jr., and W. M. Thompson, "Ascites or pleural effusion? CT differentiation: Four useful criteria," *RadioGraphics*, vol. 6, pp. 135–149, 1986.